HEALTH PHYSICS

OFFICIAL JOURNAL OF THE HEALTH PHYSICS SOCIETY

Volume 2

KARL Z. MORGAN
Editor-in-Chief

W. S. SNYDER   J. A. AUXIER
Editors

PERGAMON PRESS   NEW YORK LONDON

Los Alamos
Scientific Laboratory

MAR 28 1962

Libraries
Property

ACCIDENTAL RADIATION EXCURSION AT THE OAK RIDGE Y-12 PLANT—III

DETERMINATION OF RADIATION DOSES

G. S. HURST, R. H. RITCHIE AND L. C. EMERSON

Health Physics Division, Oak Ridge National Laboratory,* Oak Ridge, Tennessee

I. INTRODUCTION

AN analysis of the physical events leading to an accidental radiation excursion at the Oak Ridge Y-12 Plant has been presented in the first of this series of articles.[1] A companion article[2] is devoted to health physics problems arising from this accident. The present article describes the methods which were used to arrive at the doses received by the individuals. Although our main objective is to describe the dose analysis of this particular excursion, efforts will be made to present methods and information which may be of use in similar problems.

Very early estimates of the doses received by the individuals, based on their known positions at the initiation of the excursion and an estimate of the total number of fissions in the assembly, were unreasonably high. For example, the fast neutron component of the total dose received by employee A was estimated to have been 1500 rads. Hence one must assume that the location of personnel during a substantial fraction of their exposure time is unknown. This fact, together with the fact that the exposed employees were not wearing any type of personnel monitoring equipment, dictates that the evaluation of dose be based on the activation of body elements. Experience at Los Alamos[3] in the Pajarito accident indicates that of the body fluid methods, Na^{24} in blood may be the most reproducible criterion of neutron exposure and, in particular, indicates that the formation of P^{32} in urine is poorly understood.

In spite of the fact that the exposed individuals were wearing no dose-measuring devices,† it is believed that the final dose values are reasonably accurate (± 20 per cent). The doses were arrived at by the following procedure: (1) Blood and urine samples were collected from the exposed employees; these samples were counted for radioactive substances‡ (Na^{24} in the blood and P^{32} and Na^{24} in the urine) as described in Section V. (2) A burro was exposed to a mock-up of the liquid assembly to determine the relationship of Na^{24} activity in the blood and neutron dose. The ratio of γ-dose, D_γ, to neutron dose, D_n, for this particular type of critical assembly was also determined with the mock-up experiment (see Section IV). (3) A parallel program calculated these same two quantities. The calculations, described in Sections II and III, proved to be extremely helpful since they provided a basis for checking the experimental procedure at various stages.

II. SODIUM ACTIVATION OF HUMAN BLOOD

The (n,γ) process in Na^{23} gives rise to Na^{24} which has a half-life of 14.8 hr and emits a 1.38 MeV γ-ray in cascade with a 2.76 MeV

---

† The personnel security badge did contain strips of indium which proved invaluable in separating the exposed from the non-exposed persons.

‡ Because of complex physiological factors involved in the interpretation of P^{32} activity in urine, this work will deal almost entirely with the interpretation of Na^{24} activity in blood. Both P^{32} and Na^{24} in urine were analyzed by L. B. FARABEE, ORNL. In the case of Na^{24} in urine, it appears possible to correlate activity with neutron dose, particularly if the first void after exposure is not used and if samples are collected before new sodium is given to the exposed individual. In the case of P^{32}, the difficulties reported in Ref. 3 were encountered.

1

γ-ray per Na^{24} decay. One expects that the cross-section for this process will follow a $1/v$ behavior from the thermal region to about 300 eV. The capture contribution of the resonance at 2.94 keV has been estimated by GOLDSTEIN[4]. He finds a very narrow resonance with a maximum cross-section at resonance of only 1 barn. It is easy to show that the number of captures occurring in this resonance is negligible compared with those occurring at thermal energies for slowing-down spectra typical of hydrogenous media. GOLDSTEIN notes that some uncertainty exists in his estimate of the resonance cross-section and that further experimental work will be necessary to resolve the uncertainty. However, it is expected that the neglect of epithermal activation of Na^{23} is not serious and this approximation will be made throughout this paper.

The human body is several mean free paths thick for fast neutrons. Consequently, the probability that a fast neutron will be captured as a thermal neutron is not very sensitive to its initial energy. Thus the body is roughly equivalent to the "long counter"[5] used so much in neutron flux measurements. The activation of elements in the blood should be a valid measure of the average thermal flux throughout the body and hence of the total flux incident at all energies.

This assumption is basic to the procedure described below for calculating the dose to those exposed in the nuclear excursion. The

Na^{24} activation ($\mu c/cm^3$) of blood in the human body will be calculated under the assumption that the body is equivalent to a cylindrical phantom of 15 cm radius composed of soft tissue.

Calculations have been made by SNYDER and NEUFELD[6] of the depth distribution of thermal neutrons in an infinite slab of tissue-equivalent material 30 cm thick due to a monoenergetic broad beam irradiation by normally incident fast neutrons. The thermal neutron flux distribution is proportional to the curves labelled T_p in Figs. 1 through 11 of SNYDER and NEUFELD[6]. From these curves one may obtain the fraction of those neutrons entering the phantom which are captured at thermal energy. This fraction is plotted in Fig. 1 as a function of the incident neutron energy. Also plotted are values for the fraction $\xi(E)$ captured in a right cylinder of 15 cm radius, obtained from the slab data by making approximate corrections for thermal and fast leakage through the surface of the cylinder. The fast leakage was calculated by simply averaging over the path length distribution in a cylinder irradiated normal to its axis, taking the attenuation kernels for plane slab penetration from the data given by SNYDER and NEUFELD[6]. The thermal leakage was determined by applying one velocity diffusion theory to those neutrons which have entered the thermal region while in the cylinder. More accurate calculations of the capture fraction for a cylindrical phantom are

being carried out by W. S. Snyd tic methods.

One may obtain an estim activity, engendered in a cyli by a beam of fast neutrons of e normal to the axis of the cylind the number of neutrons in the dE at E striking the cylinde where $\phi(E)dE$ is the fast neutron in the energy interval dE at E, t time, and A_p is the area of the c on a surface normal to the be number striking, a fraction $\xi(E$ in the phantom and the fractic will undergo capture in th process is Σ_{Na}/Σ_t, where Σ_{Na} is absorption cross-section of Na Σ_t is the total absorption cros the total number of Na^{24} ato the phantom as a result of ir given by

$$A_p \frac{\Sigma_{Na}}{\Sigma_t} t \int_0^\infty \xi(E)\phi($$

If the volume of the cylind disintegration constant of Na^2 Na^{24}), then the total Na^{24} volume, $\mathscr{A}$, induced in the flux $\phi(E)$ will be

$$\mathscr{A} = (A_p/V)(\Sigma_{Na}/\Sigma_t)\lambda t \int_0^\infty \xi$$

The total fast neutron first associated with the beam is $$\int_0^\infty D_0(E)t\phi(E)\,dE, \quad \text{where} \quad D_0$$ collision soft tissue dose in rads flux.[7]

Hence $(D_n/\mathscr{A})$, the total neutron dose received by the activation of Na^{23} due to a f energy like $\phi(E)$, is given by

$$\frac{D_n}{\mathscr{A}} = \frac{\int_0^\infty D_0(E)\phi(E}{\dfrac{A_p}{V}\dfrac{\Sigma_{Na}}{\Sigma_t}\lambda \int_0^\infty \phi(E)}$$

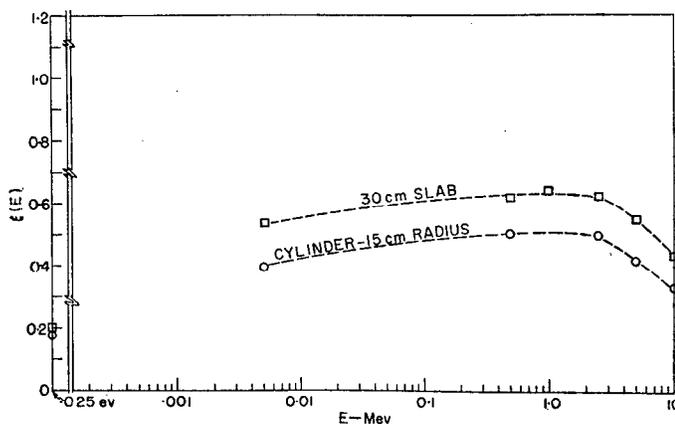The V/A_p applies to a cylind radius. The cross-section Σ

FIG. 1. Thermal neutron capture probability in a phantom.

being carried out by W. S. Snyder, using stochastic methods.

One may obtain an estimate of the Na^{24} activity, engendered in a cylindrical phantom by a beam of fast neutrons of energy E incident normal to the axis of the cylinder, by noting that the number of neutrons in the energy interval dE at E striking the cylinder is $A_p t \phi(E) dE$, where $\phi(E) dE$ is the fast neutron flux (n/cm²-sec) in the energy interval dE at E, t is the irradiation time, and A_p is the area of the cylinder projected on a surface normal to the beam. Of the total number striking, a fraction $\xi(E)$ will be captured in the phantom and the fraction of these which will undergo capture in the $Na^{23}(n,\gamma)Na^{24}$ process is Σ_{Na}/Σ_t, where Σ_{Na} is the macroscopic absorption cross-section of Na^{23} in tissue, and Σ_t is the total absorption cross-section. Hence the total number of Na^{24} atoms appearing in the phantom as a result of irradiation will be given by

$$A_p \frac{\Sigma_{Na}}{\Sigma_t} t \int_0^\infty \xi(E) \phi(E) \, dE.$$

If the volume of the cylinder is V and the disintegration constant of Na^{24} is $\lambda(\mu c$/atom of Na^{24}), then the total Na^{24} activity per unit volume, $\mathscr{A}$, induced in the phantom by the flux $\phi(E)$ will be

$$\mathscr{A} = (A_p/V) \, (\Sigma_{Na}/\Sigma_t) \, \lambda t \int_0^\infty \xi(E) \, \phi(E) \, dE. \quad (1)$$

The total fast neutron first collision dose, D_n, associated with the beam is given by $D_n = \int_0^\infty D_0(E) t \phi(E) \, dE$, where $D_0(E)$ is the first collision soft tissue dose in rads per unit incident flux.[7]

Hence $(D_n/\mathscr{A})$, the total first collision fast neutron dose received by the phantom per unit activation of Na^{23} due to a flux distributed in energy like $\phi(E)$, is given by

$$\frac{D_n}{\mathscr{A}} = \frac{\int_0^\infty D_0(E)\phi(E) \, dE}{\dfrac{A_p}{V} \dfrac{\Sigma_{Na}}{\Sigma_t} \lambda \int_0^\infty \phi(E)\xi(E) \, dE}. \quad (2)$$

The V/A_p applies to a cylinder with a 15 cm radius. The cross-section Σ_t was calculated

from the elemental abundance in the standard man[7] and is equal to 0.02339 cm⁻¹, assuming unit density for the body. Σ_{Na} was calculated using an average[8] value of 83 mequiv/l. or 1.906 mg of Na^{23} per cm³ of whole blood and an absorption cross-section of 0.536 barns.[9] One finds, approximately

$$\frac{D_n}{\mathscr{A}} \cong 5.9 \times 10^{13} \frac{\int_0^\infty D_0(E)\phi(E) \, dE}{\int_0^\infty \xi(E)\phi(E) \, dE}$$

$$\text{(rad/}\mu\text{c per cm}^3\text{)}. \quad (3)$$

It has been assumed throughout all of the work reported here that the spectrum of neutrons and γ-rays in the neighborhood of the reactor is independent of distance from the critical assembly. This is thought to be a reasonable assumption for the range of distances involved. Then one may write that the flux $\phi(E)$ at a distance R from the assembly is given by $\phi(E,R) = N(E)/4\pi R^2$, where $N(E)$ is the number of neutrons with energy E per unit energy interval leaking from the assembly.

Clearly, the replacement of the body by a cylindrical phantom for the purpose of calculation is accompanied by some uncertainties. One must assume (a) that the blood is uniformly distributed throughout the body and hence takes on a sensible average activation and (b) that the geometrical differences between the human body and the cylindrical phantom are negligible with respect to the thermal capture of incident fast neutrons. It is believed that the approximations involved will not lead to serious error in the result.

The Na^{24} method of determining the fast neutron dose is most useful in cases where the number of thermal neutrons is not large compared with the number of fast neutrons. If the number of thermals is comparatively large, the bulk of the activation will be due to neutrons which do relatively little damage to the body and the accuracy of the method will suffer. However, if the spectral distribution of neutrons is well known, one may still derive an accurate dose value. In most cases of interest to the health physicist the thermal flux component will be small enough that the Na^{24} activation may

III. CALCULATION OF D_γ/D_n FOR LIQUID ASSEMBLIES

Following the accident it seemed desirable to estimate the leakage spectra of the neutrons and the γ-rays. The overall accuracy of the methods employed in the case of the fast neutron leakage is not easy to assess in view of the rather complicated geometry of the assembly and surrounding materials but the calculated spectrum seems to agree reasonably well with the measured spectrum. A more accurate calculation is planned, in which stochastic methods will be employed.

The neutron and gamma ray leakage spectra were calculated under the assumption that the assembly could be considered spherical and the distribution of nascent fission neutrons in the assembly could be adequately represented by the fundamental spatial mode for a spherical reactor, i.e. proportional to $1/r \sin \pi r/r_0$, where r is the distance from the center of the assembly and r_0 is the radius of the equivalent sphere at the prompt critical stage (24.25 cm). The number of neutrons and γ-rays escaping the assembly was calculated by using infinite medium penetration data for point isotropic sources and by integrating these data over the volume source distribution assumed. This approximate procedure of employing infinite medium attenuation data is dictated by the lack of information relative to the bounded medium. The error involved in this procedure is believed to be small.

The details of calculation of the neutron escape spectrum will now be described. The escape of high energy neutrons ($E > 0.5$ MeV) from the assembly was carried out using infinite medium penetration data for fission neutrons in water.[10] One fits $\psi(E,r)$, the flux of neutrons of energy E at a distance r in water from a unit point source of fission neutrons, by an expression of the form,

$$\psi(E, r) = \frac{1}{4\pi r^2} \sum_i A_i(E) \exp\left(-r\mu_i(E)\right) \quad (4)$$

where the constants $A_i(E)$ and $\mu_i(E)$ are determined from an empirical fit to the data.
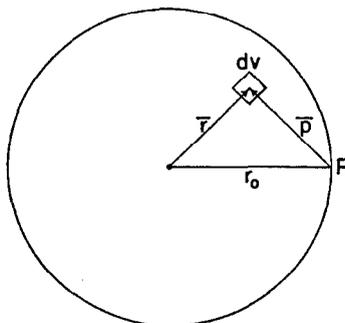

FIG. 2. Geometry used in calculating sphere transmission factors.

In all cases considered, only a few terms in the series were needed to obtain a good fit to the data. Then, one needs to calculate the leakage fraction through the surface at r_0 for a general attenuation kernel proportional to $e^{-\mu r}/4\pi r^2$ in order to determine the leakage fraction for the normalized distribution $\mathscr{S}(r)$ inside the sphere. The leakage fraction $\mathscr{L}$ through the surface is given by

$$\mathscr{L} = 4\pi r_0^2 \int dv \frac{e^{-\mu p}}{4\pi \mathbf{p}^2} \cos \varphi \mathscr{S}(r) \quad (5)$$

where $\mathbf{p}$ is a vector to the volume element dv from the point P on the surface and $\cos \varphi$ is the angle between $\mathbf{p}$ and the inward normal to the surface at P (see Fig. 2). The integration is carried out over the interior of the sphere. Integrating over the volume by first varying $\mathbf{p}$ while holding r constant and then finally integrating over r, one finds

$$\mathscr{L}(\mu r_0) = \frac{1}{4r_0^2} \int_0^{r_0} r \, dr \mathscr{S}(r) \Big\{ [r_0 + r]$$
$$\times E_2[\mu(r_0 - r)] - [r_0 - r]$$
$$\times E_2[\mu(r_0 + r)] + \frac{1}{\mu r_0}$$
$$\times [\exp\left(-\mu(r_0 - r)\right) - \exp\left(-\mu(r_0 + r)\right)]\Big\}$$

where

$$E_2(x) = \int_1^\infty \frac{du}{u^2} e^{-xu}.$$
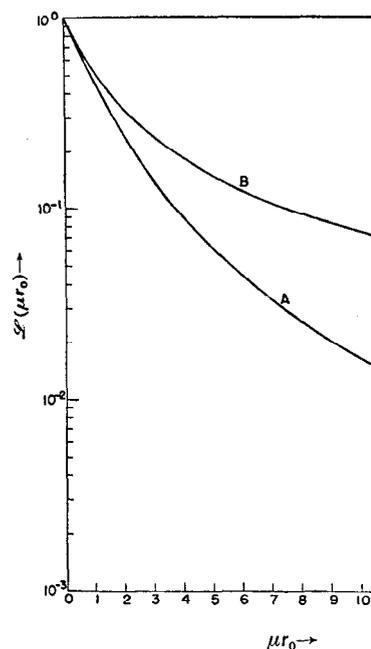
FIG. 3. Sphere transmission fac[tor] exponential attenuation kernel. C[urve A is for] a source distributed as $1/4\pi r$[...] Curve B is for a uniform source[...]

The leakage fraction $\mathscr{L}_A(\mu r_0)$ for t[he] critical mode

$$\mathscr{S}(r) = \frac{1}{4\pi r_0^2 r} \sin \frac{\pi r}{r_0}$$

was evaluated by numerical inte[gration] given as curve A of Fig. 3.

Then the leakage spectrum $N($[E] of energy E is given by

$$N(E) = \sum_i A_i(E) \mathscr{L}_A[r_0 \mu]$$

The attenuation data were fit[ted] energies and the values of A_i substituted in this equation. [...] shown in Fig. 4. Note that the [...] in this figure refers to one fissi[on] rather than to one neutron so [...] obtained from this formula have b[een] by 2.47 neutrons/fission to obtain [...] the results of ARONSON et al.[10] are [...] relatively high energies, it was [...]
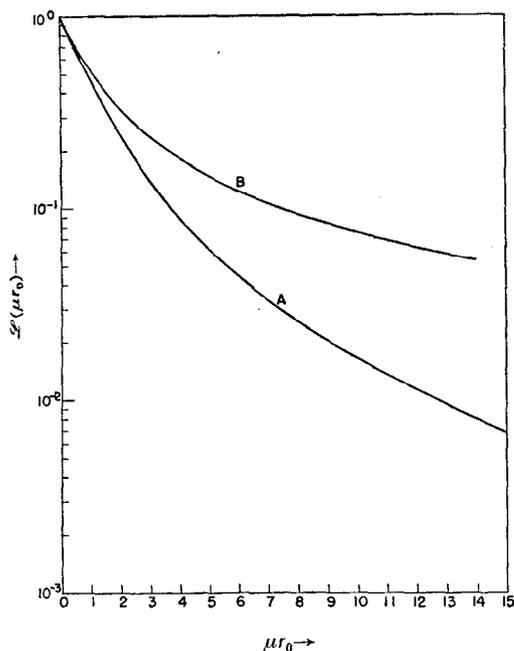
FIG. 3. Sphere transmission factors for an exponential attenuation kernel. Curve A is for a source distributed as $1/4\pi r_0^2 r\,(\sin \pi r/r_0)$. Curve B is for a uniform source distribution.

The leakage fraction $\mathscr{L}_A(\mu r_0)$ for the normalized critical mode

$$\mathscr{S}(r) = \frac{1}{4\pi r_0^2 r}\sin\frac{\pi r}{r_0}$$

was evaluated by numerical integration and is given as curve A of Fig. 3.

Then the leakage spectrum $N(E)$ for neutrons of energy E is given by

$$N(E) = \sum_i A_i(E)\mathscr{L}_A[r_0\mu_i(E)]. \qquad (7)$$

The attenuation data were fitted at several energies and the values of A_i and μ_i were substituted in this equation. The result is shown in Fig. 4. Note that the normalization in this figure refers to one fission in the core rather than to one neutron so that the data obtained from this formula have been multiplied by 2.47 neutrons/fission to obtain $N(E)$. Since the results of ARONSON et al.[10] are valid only for relatively high energies, it was necessary to
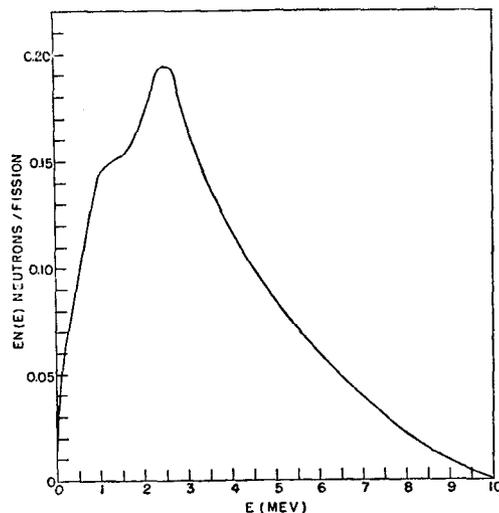

FIG. 4. Neutron leakage spectrum.

supplement them by independent calculations in the low energy region.

A multigroup, multiregion reactor analysis IBM-704 code[11] applicable to water moderated systems was available and was used for this purpose.* Since this code is limited to a constant extrapolation distance (independent of energy group), two independent calculations were made, one with an extrapolation length found from an overall group average, and the other with a value appropriate to the high energy region. The leakage in the high energy region predicted by the second calculation was not inconsistent with the results obtained from the infinite medium attenuation kernels. However, since the leakage spectrum was given rather incompletely in this range of energies by this particular multigroup code and since the diffusion approximations are rather suspect at these energies, the attenuation kernel results were employed. The results of the first multigroup calculation of the leakage at low energies were used. The resulting estimate of the composite spectrum is shown in Fig. 4. The ordinate in this figure is $EN(E)$, where $N(E)dE$ is the total number of neutrons in dE at E leaking

---

* The writers are indebted to Mr. V. E. ANDERSON of the Numerical Analysis Group of the Oak Ridge Gaseous Diffusion Plant for carrying out this portion of the calculation.

Table 1. *Relative flux density of neutrons for various energy regions*

Energy range	(Neutrons/cm²)$_{exp.}$	Normalization	
		(Neutrons/cm²)$_{exp.}$	(Neutrons/cm²)$_{theor.}$
Thermal	0.90×10^{11}	0.45	0.08
Total fast	2.0×10^{11}	1.00	1.00
0.5 keV to 0.75 MeV	0.25×10^{11}	0.125	0.30
0.75 MeV to 1.5 MeV	0.70×10^{11}	0.35	0.204
1.5 MeV to 2.5 MeV	0.58×10^{11}	0.29	0.246
>2.5 McV	0.50×10^{11}	0.25	0.250

from the assembly per fission occurring in the interior. The total dose, $\int_0^\infty \mathcal{D}_0(E) N(E)\, dE$, in this spectrum is found to be 1.08×10^{-9} rad-cm²/fission, and the ratio $\mathcal{D}_n/\mathcal{A}$ is 1.95×10^5 rad-cm³/μc [equation (3)].

As stated above, it is assumed throughout this paper that the spectrum of escaping neutrons does not depend appreciably upon distance from the assembly, so that in equation (3) for $D_n/\mathcal{A}$ one may substitute $N(E)$ for $\phi(E)$. Although this can be only approximately true, since there is clearly an appreciable amount of scattering and degradation of the spectrum in the materials of the room, one expects that this will not lead to serious error in the dose estimates. Note that the thermal component of the calculated neutron spectrum is smaller than one finds experimentally (Table 1). The higher experimental value is probably explainable in terms of room scattering and is not inconsistent with the results of HURST, MILLS and REINHARDT* on the leakage spectrum of neutrons from the Godiva reactor.

Three sources of γ-radiation were considered in the analysis: (a) prompt γ-radiation emitted directly from the fission process, (b) capture γ-radiation resulting from (n,γ) reactions taking place within the assembly, and (c) delayed γ-radiation from the fission products contained within the assembly. The spectral distribution of the prompt γ-rays, $\Gamma(E)$, was obtained
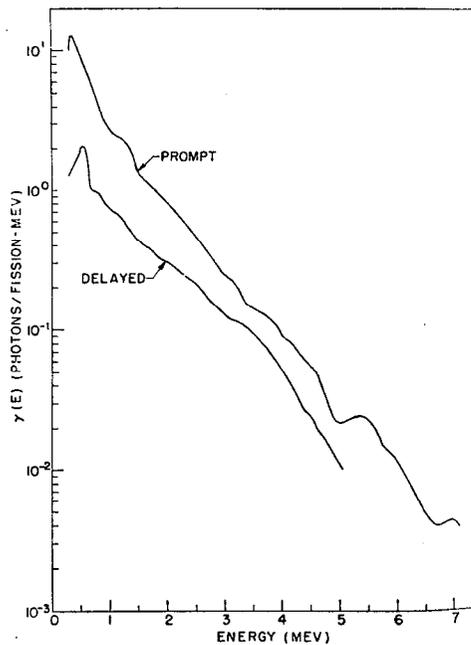
* G. S. HURST, W. A. MILLS and P. W. REINHARDT, unpublished data on neutron leakage spectrum from the Godiva reactor at LASL.

FIG. 5. Prompt and delayed γ-spectra.

directly from the recent work of MAIENSCH... et al.[12] and is shown in Fig. 5. The spat... distribution of this source is determined by t... spatial distribution of the fission events and assumed to be proportional to $1/r \sin (\pi r/...$. The capture γ-sources were obtained from t... following equation:

$$\Gamma_j = \nu\,(1 - f_e)\left(\frac{\sigma_{rc}}{\sigma_a}\right)_j \left(\frac{E_c}{E_\gamma}\right)_j \frac{(\Sigma_a)_j}{\Sigma_t}$$

Ta

Element	E_c (MeV/capt
Hydrogen	2.2
Uranium	6.8

where

Γ_j = photons of energy E_γ released ... jth element per fission;

ν = neutrons born per fission (2.4...

f_e = neutron escape fraction (0.271

σ_{rc} = microscopic radiative captu... section;

σ_a = microscopic absorption cross-s

E_c = energy release per neutron c... form of γ-rays of energy E_γ;

Σ_a = macroscopic absorption cro...

Σ_t = total macroscopic absorpti... section of the assembly.

Uranium and hydrogen were the onl... in the assembly which contributed a... to the capture γ-dose. For these ele... values for E_c and E_γ were obtai... GLASSTONE[13]. In the case of uran... values are not well known but the tot... binding energy of 6.8 MeV is acc... correctly by the proposed γ-spectr... calculated values for the capture γ-s... shown in Table 2. As in the case of t... radiation, the capture γ-rays ar... essentially simultaneously with fissi... the spatial distribution again follows... fission events.

It was not necessary to determin... plete leakage spectrum of prompt γ... fission and γ-rays from capture. One i... primarily in the γ-dose escaping t... The calculation of the leakage dose... and capture γ-rays was carried o... computing the variation of dose... distance in an infinite medium ...

Table 2. *Capture γ-ray spectra*

Element	E_c (MeV/capture)	E_γ (MeV/photon)	S (photons/fission)
Hydrogen	2.2	2.2	0.478
Uranium	6.8	3.0	0.427
		1.0	0.171

where

Γ_j = photons of energy E_γ released from the jth element per fission;

ν = neutrons born per fission (2.47);

f_e = neutron escape fraction (0.271);

σ_{rc} = microscopic radiative capture cross-section;

σ_a = microscopic absorption cross-section;

E_c = energy release per neutron capture in form of γ-rays of energy E_γ;

Σ_a = macroscopic absorption cross-section;

Σ_t = total macroscopic absorption cross-section of the assembly.

Uranium and hydrogen were the only elements in the assembly which contributed appreciably to the capture γ-dose. For these elements the values for E_c and E_γ were obtained from GLASSTONE[13]. In the case of uranium these values are not well known but the total neutron binding energy of 6.8 MeV is accounted for correctly by the proposed γ-spectrum. The calculated values for the capture γ-sources are shown in Table 2. As in the case of the prompt radiation, the capture γ-rays are released essentially simultaneously with fission so that the spatial distribution again follows that of the fission events.

It was not necessary to determine the complete leakage spectrum of prompt γ-rays from fission and γ-rays from capture. One is interested primarily in the γ-dose escaping the system. The calculation of the leakage dose for prompt and capture γ-rays was carried out by first computing the variation of dose $\mathbb{D}(r)$ with distance in an infinite medium having the composition of the assembly due to a unit point isotropic source having the indicated distribution of energy. Thus,

$$[\mathbb{D}(r)]_{\text{prompt}} = K \int_0^\infty E\Gamma(E)\mu_a{}^t(E)B_d(E,\mu r)$$

$$\times \frac{\exp(-\mu(E)r)}{4\pi r^2}\,dE \qquad (9)$$

where

$\mathbb{D}(r)$ = γ-dose at r cm from a unit source (rad/fission);

K = 1.6×10^{-8} rad/MeV-gm^{-1};

$\Gamma(E)$ = number of γ-rays of energy E emitted per unit interval from one fission (photon/fission MeV);

$\mu_a{}^t(E)$ = energy absorption coefficient for tissue dose (cm^2/g);

$B_d(E,\mu r)$ = dose buildup factor;[14]

$\mu(E)$ = attenuation coefficient of water for photons of energy E (cm^{-1}).

The integration was performed numerically using values of B_d obtained from the work of GOLDSTEIN and WILKINS[14]. $[\mathbb{D}(r)]_{\text{capture}}$ was evaluated in the same way except that a sum over the j capture photon groups was carried out. The computed curves for $[\mathbb{D}(r)]_{\text{prompt}}$ and $[\mathbb{D}(r)]_{\text{capture}}$ were then fitted by empirical formulas of the form used in the neutron calculation,

$$\mathbb{D}(r) = \frac{1}{4\pi r^2}\sum_i A_i \exp(-\mu_i r) \qquad (10)$$

and the dose, D_γ, escaping per fission was found from the equation

$$D_\gamma = \sum_i A_i \mathscr{L}_A(\mu_i r_0). \qquad (11)$$

The treatment of the delayed radiation presents somewhat more of a problem as both

the source strength and the energy distribution are strongly time dependent during the first few seconds following fission. The spectral distribution shown in Fig. 3, was obtained by normalizing the spectrum measured by MAIEN-SCHEIN et al.[12] at 6.2 sec to the integral over the first 15 sec of the measured decay spectrum. It was necessary to extrapolate to obtain values during the first second. The delayed γ-emitters were assumed to be homogeneously distributed throughout the assembly because of turbulence following the initial release of energy, hence it was necessary to obtain transmission factors for uniformly distributed sources of γ-rays. The leakage fraction, $\mathscr{L}_B(\mu r_0)$ for a normalized uniform distribution $\mathscr{S}(r) = \dfrac{3}{4\pi r_0^3}$ may be written explicitly as

$$\mathscr{L}_B(\mu r_0) = \tfrac{3}{8}(\mu r_0)^{-3} \times [2(\mu r_0)^2 - 1 + (1 + 2\mu r_0)\exp(-2\mu r_0)] \quad (12)$$

which may be shown by carrying out the integration indicated in equation (6). This result is shown as curve B of Fig. 3.

The movements of the exposed persons subsequent to the initial excursion influenced the amount of γ-radiation which they received. In the dose analysis it was assumed that each person exposed was exposed to a single nuclear excursion but that his individual actions in the few seconds following the excursion resulted in different γ-neutron dose ratios. This results in a delayed γ-dose slightly larger than that obtained by assuming a constant power assembly delivering the same total fission energy. The following three cases treated were based upon the actions of each of the individuals as determined from personal interviews.[15]

Case I (*employee* A). This employee was exposed to the full complement of prompt and capture γ-radiation but, since it is believed that he left the area first, it was assumed that only the first 5 sec of the delayed γ-spectrum contributed to his dose.

Case II (*employee* E). This employee was also exposed to the prompt and capture γ-radiation source, but the γ-neutron ratio was adjusted to take into account an assumed 15 sec exposure to the delayed γ-spectrum and, further, that his exit from the area took him to within 10 ft of

the assembly. This case gives the lar γ-neutron dose ratio used in analysis a reflects the fact that this employee was appare the last to leave the area. The assumed e path resulted in a total γ-dose which was 8 p cent more than the dose of the constant dista 15 sec exposure case. This represents what believed to be the maximum increase th could have occurred for any of the personne

Case III (*employees other than* A *and* E). The employees were assumed to have received t full contribution of prompt and capture γ-radi tion, but, like case I, the delayed γ-rays we received at a constant distance and, like case II the first 15 sec of the delay spectrum w effective.

The escaping dose from delayed γ-rays whi was received in the three cases considered w determined by the same method used the prompt and capture γ-dose calculatio The dose $[\mathbb{D}(r)]^{(J)}_{\text{delayed}}$ was found from equ (9) in which the portion of the delayed spectru $[\Gamma(E)]^{(J)}_{\text{delayed}}$ seen by the Jth case was employ $[\mathbb{D}(r)]^{(J)}_{\text{delayed}}$ was then fitted by an empiri expression having the form of equation (1 and the escaping dose $[D_\gamma]^{(J)}_{\text{delayed}}$ seen by ca J was calculated from the equation:

$$[D_\gamma]^{(J)}_{\text{delayed}} = [\sum_i A_i \mathscr{L}_B(\mu_i r_0)]^{(J)}.$$

The results for the dose multiplied by $4\pi r^2$ a shown in Table 3.

IV. DOSE MEASUREMENTS WITH A MOCK-UP OF THE CRITICAL ASSEMBLY

To establish experimentally the relations between the total (neutron + γ) first collision d and the blood Na activation, a mock-up of critical assembly was constructed and operated a low power reactor in two experiments. Fig shows the actual reactor tank surrounded with large tank which rested on a concrete floor. Table gives details of the mock-up assembly as compar to the actual critical assembly. The first experim was designed to measure the ratio of γ-dose $D_$ neutron dose D_n, i.e. D_γ/D_n. The assembly w operated at a power of about 6 W for 11 min. T γ-dose rate at 6 ft from the center of the assemb point A in Fig. 6, was measured with an ioniza

_____

* This phase of the work was carried out at the OR criticality facility.

Case no.	Prompt (rad-cm^2/fission)
I	2.06×10^{-9}
II	2.06×10^{-9}
III	2.06×10^{-9}

Table 4. Comparis

Diameter (in.)
Height (in.)
U^{235} conc. (g/l.)
Total U^{235} (kg)

chamber having carbon walls a ionization chamber was cali γ-radiation to read the first co rads. Measurements of the ne carried out at the above mentio Radsan fast neutron dosimeter absolute proportional counter.[1 measurements gave a value of 3.

The ratio $D_\gamma/D_n = 3.3$ ap which has been running at approximately 3 min, the time a the measurement was made. this result with those given in must be corrected to correspo (a) the critical assembly is instantaneous pulse of radiatic first 15 sec of the decay γ-radi effective. When the experime SCHEIN et al.[12] for the spectru are used, the experimentally de becomes 2.8 compared to th 3.09 given in Table 3.

In the second experiment critical assembly, a burro was

_____

Table 3. Results of γ-dose calculation

Case no.	Prompt (rad-cm²/fission)	Capture (rad-cm²/fission)	Delayed (rad-cm²/fission)	Total (rad-cm²/fission)	D_γ/D_n
I	2.06×10^{-9}	6.4×10^{10}	4.0×10^{-10}	3.10×10^{-9}	2.87
II	2.06×10^{-9}	6.4×10^{-10}	9.4×10^{-10}	3.64×10^{-9}	3.37
III	2.06×10^{-9}	6.4×10^{-10}	6.4×10^{-10}	3.34×10^{-9}	3.09

Table 4. Comparison of the mock-up critical assembly with the actual critical assembly

	Actual critical assembly	Mock-up critical assembly
Diameter (in.)	22	20
Height (in.)	9.2	15
U^{235} conc. (g/l.)	37.4	25.9
Total U^{235} (kg)	2.1	2.00

chamber having carbon walls and CO_2 gas.* This ionization chamber was calibrated with Co^{60} γ-radiation to read the first collision tissue dose in rads. Measurements of the neutron dose rate were carried out at the above mentioned position with the Radsan fast neutron dosimeter,[16] which uses the absolute proportional counter.[17] These two sets of measurements gave a value of 3.3 for the ratio D_γ/D_n.

The ratio $D_\gamma/D_n = 3.3$ applies for the reactor which has been running at constant power for approximately 3 min, the time after start-up at which the measurement was made. In order to compare this result with those given in Section III, this ratio must be corrected to correspond to the case where (a) the critical assembly is assumed to give an instantaneous pulse of radiation, and (b) only the first 15 sec of the decay γ-radiation is assumed to be effective. When the experimental results of MAIENSCHEIN et al.[12] for the spectrum of the decay γ-rays are used, the experimentally determined ratio, D_γ/D_n, becomes 2.8 compared to the calculated ratio of 3.09 given in Table 3.

In the second experiment with the mock-up critical assembly, a burro was exposed in such a way

that a point on his plane of symmetry coincided with the point A where the neutron dose was measured in the first experiment. The burro was chosen as the experimental animal because (a) he is a large
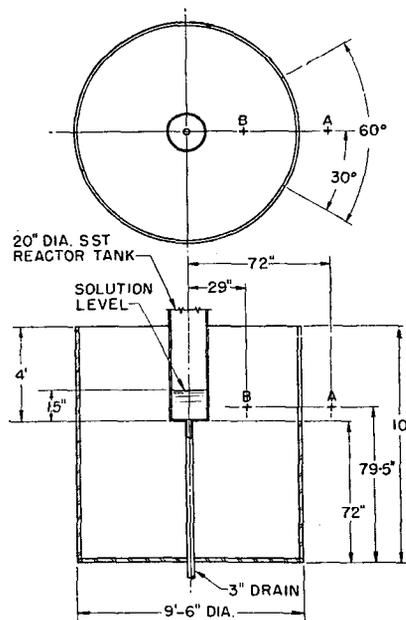
---

* This type of ionization chamber has been used extensively by the Neutron Physics Division, ORNL, in their shielding program. For a description, see L. H. BALLWEG and J. L. MEEM, Standard Gamma-Ray Ionization Chambers for Shielding Measurements. ORNL-1028.

FIG. 6. Schematic of mock-up experiment.

Table 5. Blood sodium for individuals exposed and for experimental burro

Exposed individuals	Blood sodium (mg/ml serum)
A	3.2
B	3.2
C	3.2
D	3.1
E	3.2
Experimental burro	3.1

animal comparable in size to man, and (b) the amount of sodium per gram of blood serum is approximately the same for burro and man. Table 5 shows the concentration of sodium in blood serum for the burro and for some of the exposed individuals.*

The second experiment was operated at a power of about 300 W for 42 min which gave the burro a fast neutron first collision dose of 48 rads.† Blood samples were drawn from the burro and counted for Na^{24} as described in the next section. From these data the value of $\mathscr{A}/D_n$ for this particular neutron spectrum was determined to be 6.0×10^{-6} μc of Na^{24} per ml of blood and per rad of neutron dose, compared to 5.14×10^{-6} μc obtained by using the methods given in Sections II and III. Note that the results calculated in Section II apply to the case where a model of a man is the irradiated object. The close agreement of these two values is further indication that the burro is a good phantom for a man.

Also, in the second experiment a series of threshold detectors[18,19] was used to obtain information on the fast neutron spectrum. The neutron detectors [Au (Au + Cd), S^{32} and Pu^{239}, Np^{237} and U^{238} in 2.2 g/cm² B^{10}] were exposed at approximately 29 in. from the center of the liquid assembly, point B in Fig. 6. The total flux of neutrons received during the 42 min period for various energy ranges is shown

---

* These measurements were made by Dr. C. H. STEFFEE, Oak Ridge Hospital, using the flame photometer technique. Although it was not possible to obtain whole blood sodium values at the time the experimental work was done, a subsequent evaluation of whole blood sodium for unirradiated burros showed results not inconsistent with values to be expected in normal man.

† The amount of exposure was determined with a U^{235} fission chamber which had been calibrated in terms of fast neutron dose in the first experiment.

in Table 1. The table also shows a comparison with the calculations given in Section III. Using the flux values measured at point B the first collision neutron dose can be calculated[18] at the burro exposure position (point A). A sulfur disc was fixed on the side of the burro facing the assembly. The measured value of the flux was corrected for distance and for flux build-up‡ due to the burro to obtain the flux which would have existed at point A had the burro not been there. The first collision neutron dose at point A was then determined from the ratio of the neutron flux at point A to that at point B and the neutron dose calculated for point B. Thus the threshold detector data when suitably corrected to refer to point A gives a first collision neutron dose at point A equal to 42 rads compared to 48 rads using the proportional counter method.

The value of the thermal neutron flux in Table 1 shows that the dose due to thermal neutrons is negligible compared to the fast neutron dose. However, the magnitude of the thermal neutron flux is of interest because of another factor. In Fig. 1 it is seen that the probability that a thermal neutron entering the human body will produce Na^{24} is about 0.4 as large as the probability that a fast neutron will become thermalized and produce a Na capture in the body. Thus it would be expected that for the spectrum shown in Table 1 only about 15 per cent of the Na^{24} activity would be produced by thermal neutrons. This fact is of considerable practical importance since it implies that it is not necessary to consider the spatial distribution of thermal neutrons in detail.

V. ASSIGNMENT OF DOSE VALUES TO THE EXPOSED INDIVIDUALS

The blood samples collected from the individuals were counted with a 2 × 4 in. NaI crystal (Fig. 7. Polyethylene bottles (4 fluid oz capacity) containing the whole blood were placed on the top of the crystal. The horizontal lines indicate liquid levels for 50 and 100 ml. Counting was done with a discriminator set to accept γ-rays above 0.66 MeV and 2.0 MeV. The equipment was calibrated with 50 and 100 ml solutions of Na^{24} in water. The counting geometry for Na^{24} as well as the counter background (using a 4 in. lead shield) is shown in Table 6 for the two bias values and for 50 and 100 ml samples.

A few hours after exposure, 100 ml blood samples were taken from some of the individuals, and this was counted as whole blood without the use of an anticoagulant. A second set of blood samples was

---

‡ The depth dose curves taken from W. S. SNYDER, *Brit. J. Radiol.* **28**, 342 (1955), and *NBS Handbook* 63, November 1957, were used as a basis of correction.

Table 6. Na^{24} counting geometry

Bias (MeV)	Geometry (%)
0.66	17.7
2.0	5.9

Table 7. Na^{24} ac

Exposed individuals	Na^{24} (μc/ml)	Experiment neutron dos (rad)
A	5.8×10^{-4}	96
B	4.3×10^{-4}	71
C	5.4×10^{-4}	89
D	5.2×10^{-4}	86
E	3.7×10^{-4}	62
F	1.1×10^{-4}	18
G	1.1×10^{-4}	18
H	0.36×10^{-4}	6.0
Burro	2.9×10^{-4}	48

* Using $D_\gamma/D_n = 2.8$.
† Using $D_\gamma/D_n = 3.09$.

taken about 20 hr later, but this time o was used and heparin was added to preven This set of data was more nearly uniform first and it is the basis of the final dose value The blood samples were counted for sever establish that Na^{24} was the primary isot counted. Very early counting showed som of K^{42} in the case when the counting 0.66 MeV.

Table 7 shows the final results for the Na (extrapolated to the time of exposure) for th personnel as well as that for the experimen Blood samples (100 ml) from the burro, r neutron dose of 48 rads, were counted‡ in way as described above for the exposed in Table 7 shows the first collision neu γ-dose, and total dose obtained from the exp data by direct comparison of Na^{24} activi

---

‡ For the first few hours Cl^{38} competed especially at the 0.66 MeV bias.

Table 6. Na²⁴ counting geometry and background for 2 by 4 in. NaI crystal at two bias levels

Bias (MeV)	Geometry (50 ml) (%)	Geometry (100 ml) (%)	Background (counts/min)
0.66	17.7	13.3	250
2.0	5.9	4.3	115

Table 7. Na²⁴ activation and dose values for exposed personnel

Exposed individuals	Na²⁴ (μc/ml)	Experimental neutron dose (rad)	Theoretical neutron dose (rad)	Experimental* γ-dose (rad)	Theoretical† γ-dose (rad)	Total experimental dose (rad)
A	5.8×10^{-4}	96	113	269	349	365
B	4.3×10^{-4}	71	83	199	256	270
C	5.4×10^{-4}	89	104	250	321	339
D	5.2×10^{-4}	86	100	241	308	327
E	3.7×10^{-4}	62	72	174	223	236
F	1.1×10^{-4}	18	21	50.5	64.9	68.5
G	1.1×10^{-4}	18	21	50.5	64.9	68.5
H	0.36×10^{-4}	6.0	7.0	16.8	21.6	22.8
Burro	2.9×10^{-4}	48				

* Using $D_\gamma/D_n = 2.8$.
† Using $D_\gamma/D_n = 3.09$.

taken about 20 hr later, but this time only 50 ml was used and heparin was added to prevent clotting. This set of data was more nearly uniform than the first and it is the basis of the final dose values reported. The blood samples were counted for several days to establish that Na²⁴ was the primary isotope being counted. Very early counting showed some evidence of K⁴² in the case when the counting bias was 0.66 MeV.

Table 7 shows the final results for the Na²⁴ activity (extrapolated to the time of exposure) for the exposed personnel as well as that for the experimental burro. Blood samples (100 ml) from the burro, receiving a neutron dose of 48 rads, were counted‡ in the same way as described above for the exposed individuals.

Table 7 shows the first collision neutron dose, γ-dose, and total dose obtained from the experimental data by direct comparison of Na²⁴ activities in the human blood with that of the burro blood, using the known fast neutron dose given to the burro and the experimentally measured ratio, D_γ/D_n. Also shown in Table 7 are the dose values obtained by calculations, Sections II and III.§

The counting methods described above are very sensitive. For example, it is seen by using data from Tables 6 and 7 that 1 rad of neutrons give a count rate due to Na²⁴ equal to 40 counts/min (at zero time) for 50 ml burro blood when the counting bias is 2.0 MeV. Thus, since the counter background rate is 115 counts/min, a dose of 1 rad can be detected. With minor improvements in counting techniques, it should be possible to determine doses as low as 100 mrads with the Na²⁴ method.

‡ For the first few hours Cl³⁸ competed with Na²⁴, especially at the 0.66 MeV bias.

§ The calculated values given in the table differ from the corresponding values in report Y-1234, *Accidental Excursion at the Y-12 Plant*, (4, August 1958). The inadvertent use of a high value of the concentration of Na²³ in whole blood gave calculated values which were too low.
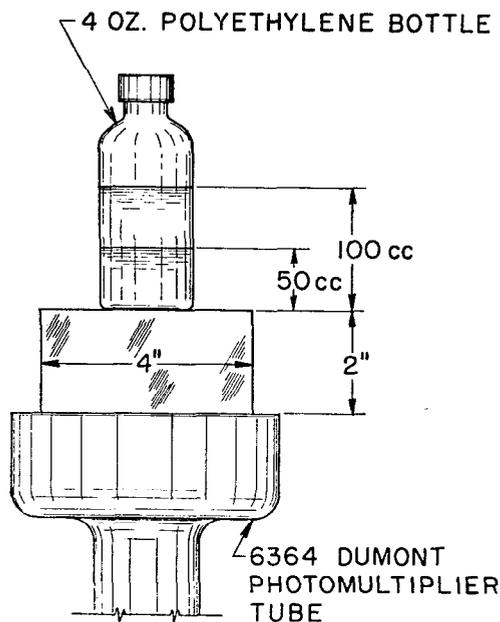
FIG. 7. Geometry of the blood counter.

VI. DISCUSSION OF ERRORS

As mentioned in Section I, comparison of calculations with experiment leads to independent tests of some of the assumptions made in the experimental program. The various sources of error in the experimental approach and the extent to which comparison of theory and experiment helps to decrease the uncertainty involved in individual assumptions will now be summarized. The assumptions made in the experimental program are:

(1) The actual radiation spectrum is duplicated with the mock-up reactor.

(2) Na^{24} activity in blood of the exposed person is approximately proportional to the first collision neutron dose, i.e. the Na^{24} activity resulting from capture of thermal neutrons coming from the reactor constitutes a correction factor.

(3) The relationship of Na^{24} activity in the blood of a burro, exposed to the radiation from the mock-up reactor, to the first collision dose is valid for a man exposed to the actual radiations.

(4) The γ-dose for each of the exposed

persons may be established by determining the ratio D_γ/D_n for the mock-up facility.

Assumption (1) was checked by measuring the neutron leakage spectrum from the mock-up with threshold detectors. The neutron leakage spectrum from the actual assembly was calculated. Table 1 shows comparison of these two spectra. The γ-spectrum for the actual assembly was calculated with what is thought to be reasonable accuracy. Errors in dose due to the difference in spectra were thought to be negligible.

Assumption (2) may lead to error for some of the cases. It was shown by calculation (see Fig. 1) that thermal neutrons are less effective than fast neutrons in producing Na^{24} in the blood. Measurements of the thermal neutron flux for the exposed burro combined with this result show that only about 20 per cent of the Na^{24} is due to thermal neutrons coming directly from the reactor. However, for those persons at large distances from the reactor, the Na^{24} method may lead to overestimates of the dose. This point deserves further exploration.

Assumption (3) was checked by comparison with calculation. The relationship of neutron dose to Na^{24} activity was calculated for a man exposed to the neutron spectrum, found from calculations on the actual assembly, and compared to the value for a burro exposed to the mock-up. The value of rad per μc per ml of blood was 20 per cent higher for the calculated case.

Assumption (4) has already been considered in detail in Section III. Very little error results from this assumption.

REFERENCES

1. D. CALLIHAN and J. THOMAS, (1959).
2. J. D. MCLENDON, *Health Phys.*
3. J. G. HOFFMAN, *Radiation Dc Accident of May* 21, 1946. LA-(
4. H. GOLDSTEIN, *The Attenuatio and Neutrons in Reactor Shields.* 1
5. A. O. HANSON and J. L. McI **72,** 673 (1947).
6. W. S. SNYDER and J. NEUFEL **28,** 342 (1955).
7. *National Bureau of Standards H* (1957).

exposed persons was determined by Dr. C. H. STEFFEE, Oak Ridge Hospital. We would also like to thank the entire ORNL criticality group for their work in designing and operating the mock-up reactor experiments and the University of Tennessee AEC Agricultural Research Program for the work associated with the use of the burro. We are also pleased to acknowledge continued guidance and suggestions from K. Z. MORGAN, H. P. YOCKEY and M. J. COOK. To the many others who were called upon to render services in their fields of speciality, we also extend our thanks.

REFERENCES

1. D. CALLIHAN and J. THOMAS, *Health Phys.* **1,** 363 (1959).
2. J. D. McLENDON, *Health Phys.* **2,** 21 (1959).
3. J. G. HOFFMAN, *Radiation Doses in the Pajarito Accident of May* 21, 1946. LA-687 (1948).
4. H. GOLDSTEIN, *The Attenuation of Gamma Rays and Neutrons in Reactor Shields.* NYO-6269 (1957).
5. A. O. HANSON and J. L. McKIBBEN, *Phys. Rev.* **72,** 673 (1947).
6. W. S. SNYDER and J. NEUFELD, *Brit. J. Radiol.* **28,** 342 (1955).
7. *National Bureau of Standards Handbook* 63 Fig. 1 (1957).
8. W. S. SPECTOR, *Handbook of Biological Data.* Saunders, Philadelphia (1956).
9. D. J. HUGHES and J. A. HARVEY, *Neutron Cross Sections.* BNL-325 (1955).
10. R. ARONSON, J. CERTAINE, H. GOLDSTEIN and S. PREISER, *Penetration of Neutrons from a Point Isotropic Fission Source in Water.* NYO-6267 (1957).
11. C. L. DAVIS, J. M. BOOKSTON and B. E. SMITH, *GNU II—A Multigroup One-Dimension-Diffusion Program.* GMR-101 (1957).
12. F. C. MAIENSCHEIN, R. W. PEELLE, W. ZOBEL and T. A. LOVE, *Second United Nations International Conference on the Peaceful Uses of Atomic Energy* Paper A/Conf. 15/P/670 (1958).
13. S. GLASSTONE, *Principles of Nuclear Reactor Engineering.* Van Nostrand, New York (1955).
14. H. GOLDSTEIN and J. E. WILKINS, *Calculations of the Penetrations of Gamma Rays.* NYO-3075 (1954).
15. *Accidental Radiation Excursion at the Y-12 Plant,* Y-1234 (1958).
16. E. B. WAGNER and G. S. HURST, *Rev. Sci. Instrum.* **29,** 153 (1958).
17. G. S. HURST, *Brit. J. Radiol.* **27,** 353 (1954).
18. G. S. HURST, J. A. HARTER, P. N. HENSLEY, W. A. MILLS, M. SLATER and P. W. REINHARDT, *Rev. Sci. Instrum.* **27,** 153 (1956).
19. P. W. REINHARDT and F. J. DAVIS, *Health Phys.* **1,** 169 (1958).